International Journal of Recent Technology and Engineering (IJRTE)
ISSN: 2277-3878 (Online), Volume-13 Issue-2, July 2024

Impact of Irradiance and Temperature on Electrical Parameters of Polycrystalline Photovoltaic Module: A Five Parameter Analysis

Chandrashekhar Pardhi, Kanchan Khare, Ashish Choubey

Abstract: ***In the current era, adopting renewable energy is not just a choice but a necessity. The role of photovoltaic modules significantly influences this shift from conventional energy sources. The performance and parameters of these PV cells are greatly affected by both irradiance and temperature. While the standard test condition assumes 1000 watts/m² and 25°C temperature, the reality of solar geometry often alters these values, leading to changes in the electrical parameters of the PV cell. This study, which employs a five-parameter single-diode model, is of paramount importance in understanding the impact of irradiance and temperature. The parameters are extracted from the P-V and I-V curves of the simulated solar cell and matched with data from the TP300 series polycrystalline TATA Power solar module. The analysis across various temperature and irradiance levels provides crucial insights into changes in shunt and series resistance, diode ideality factor, reverse saturation current, and photo-generated current. This investigation is vital in understanding how parameter alterations correlate with changes in solar cell performance. The study uses the MATLAB Simulink platform, utilizing data from the TATA solar module TP-300 series datasheet.***

Keywords: Photovoltaic Module, Irradiance, Temperature, Shunt Resistance, Series Resistance, Diode Ideality Factor, Reverse Saturation Current, Photogenerated Current.

I. INTRODUCTION

As the world grapples with the looming energy crisis, the transition to renewable energy sources has emerged as the most promising solution, offering both sustainability and a cleaner environment. Solar and wind power stand at the forefront of this global movement, championed by nations worldwide. India, in particular, has made significant strides, boasting a total installed capacity of over 60GW in photovoltaic plants, placing it among the top five nations globally in solar power adoption.

Manuscript received on 18 May 2024 | Revised Manuscript received on 28 May 2024 | Manuscript Accepted on 15 July 2024 | Manuscript published on 30 July 2024.
*Correspondence Author(s)
Chandrashekhar Pardhi, Department of Electrical Engineering, Jabalpur Engineering College, Jabalpur, (M.P.), India, E-mail ID: shriradhavallabha17@gmail.com ORCID ID: 0009-0000-6460-3060
Kanchan Khare, Department of Applied Chemistry, Jabalpur Engineering College, Jabalpur, (M.P.), India, E-mail ID: kkhare@jecjabalpur.ac.in, ORCID ID: 0000-0001-5357-1569
Ashish Choubey*, Department of Electrical Engineering, Jabalpur Engineering College, Jabalpur, (M.P.), India, E-mail ID: aschoubey@jecjabalpur.ac.in, ORCID ID: 0009-0008-3850-9407

The Indian government is fervently promoting renewable energy installations to foster a greener energy landscape and reduce reliance on conventional sources. Solar energy, with its versatile applications spanning domestic lighting, village electrification, water pumping, railway signals, and remote telecommunication, holds immense promise. With decreasing solar costs and escalating grid power prices, India's solar power capacity is poised for substantial growth [1][27][28].

Photovoltaic materials primarily consist of polycrystalline, monocrystalline, and amorphous silicon. Polycrystalline silicon exhibits heightened sensitivity to temperature variations and possesses a short life span, resulting in lower efficiency typically ranging between 12-15%. In contrast, although pricier, monocrystalline silicon boasts an extended lifespan and higher efficiency spanning between 15-25% compared to other materials. Amorphous silicon, known as thin film, offers an efficiency range similar to polycrystalline silicon at 12-15%, characterized by its lower cost and shorter life span. The superior longevity of monocrystalline modules, particularly evident across diverse atmospheric conditions, stems from their impeccable lattice structure, heightened material purity, minimal grain boundary energy, and reduced internal resistance, distinguishing them from polycrystalline modules [2].

Due to its accuracy, the single-diode model often called the five-parameter model, is the preferred choice for modeling solar cells. Renowned for its precision, the five-parameter model is widely adopted by researchers and authors alike for performance analysis purposes. This model focuses on five essential parameters crucial for solar cell characterization: shunt resistance (R_{sh}),series resistance (R_s), diode ideality factor (η); diode reverses saturation current (I_o), and photo-generated current (I_{ph}). These parameters are typically extracted from the I-V characteristics provided by the manufacturer's datasheet [3]. The efficiency of the single-diode model for photovoltaic cells is contingent upon solar radiation and operating temperature, given the direct influence of these conditions on model parameters [4]. Numerous methods have been proposed for parameter extraction, including efficient iterative, curve fitting, iterative five-point, analytical five-point, hybrid, and combined analytical-numerical approaches [5,6,7,8]. An appropriate solar panel can be selected for any application based on the information provided by the manufacturer's datasheet. This includes the type of solar material (polycrystalline /monocrystalline) and the maximum power output. P_m, corresponding maximum output voltage V_{mp} and maximum output current I_{mp}.

Additionally, the datasheet provides the ratings of open circuit voltage V_{oc}, short circuit current I_{sc}, open circuit voltage temperature coefficient K_v, and short circuit current temperature coefficient K_i. Information regarding the configurations of solar cells connected in series and parallel for rated output is also specified. These details are typically provided at the standard test conditions (STC), comprising an irradiance level of 1000 W/m², cell temperature of 25°C, and spectral distribution of air mass of 1.5. Furthermore, the datasheet includes output curves P-V and I-Vat standard test conditions (STC) as well as at normal operating test conditions (NOCT), the latter representing 800 W/m² irradiance level and cell temperature 20°C. Such comprehensive information aids in modeling the solar module and understanding its performance under varying atmospheric conditions [9]. In the five-parameter model of solar cells, the output is contingent upon the five parameters, which are influenced by atmospheric conditions. Irradiance and cell temperature changes consequently impact these parameters, leading to fluctuations in output and efficiency. To achieve this objective, data is sourced from the datasheet of Tata Solar power TP 300 series polycrystalline photovoltaic module at standard test conditions. Utilizing the MATLAB Simulink PV array block, the current-voltage (I-V) and power-voltage (P-V) curves are generated.

The five parameters of the single diode model are then determined using the key performance metrics at standard operating conditions (STC). Subsequently, five different values of temperature and irradiance, ranging from 10–70 °C and 200–1000 W/m², respectively, are employed. Salient operating points of photovoltaic modules, such as V_{oc}(Open circuit voltage), I_{sc}(Short circuit current), P_{mpp} (Maximum power point), V_{mp}(the voltage at Maximum power point) and I_{mp} (Current at Maximum power point) are obtained. Leveraging these operating points across the specified temperature and irradiance range, MATLAB Simulink PV array block furnishes the five electrical parameters. This enables their detailed analysis of variations are analyzed under each operating point.

II. POLYCRYSTALLINE SOLAR CELL MATERIAL

Solar panel is an electronic equipment that uses solar radiation to produce heat or electricity. The ones that produce heat are solar thermal panels, while those that produce electricity are photovoltaic solar panels. Photovoltaic solar panels are divided into two main categories: one is monocrystalline solar panels, and the second is polycrystalline solar panels. Both monocrystalline and polycrystalline silicon are used for PV panels, but currently, polycrystalline silicon material is used with an increasing share because of the higher cost reduction potential. The second-generation solar cells as polycrystalline thin films are the current focus to meet the global clean energy demand. The silicon material is used with an increasing share as it is the only material from the other classical materials (Al, Cd, Cu, As, Ga, In, Pb, Ni) and is by far the most common semiconductor material used in solar cells [10]. Polycrystalline solar panels have solar cells made from multiple fragments of silicon crystals melted together. They are dark blue and squared structured. The efficiency of polycrystalline solar panels varies between 14% to 20%, with a life span of 25 to 35 years. Polycrystalline panels have less cost per watt, making them cheaper than the monocrystalline type, and the manufacturing process creates less waste and uses less energy, resulting in less production cost, which somehow curtails its other drawbacks in comparison to monocrystalline solar panels. The fill factor of solar cells depends on the structure and type of semiconductors, the level of doping of the two areas in a P-N junction, the amount of built-in potential barriers, and junction temperature [11]. Polycrystalline silicon is used today for many thin film applications such as silicon gate transistors, non-volatile memories, passive resistors, bipolar transistors, diodes, dynamic excesses memory, and micromechanical systems [12].

Although crystalline silicon is not the optimal material from the solid-state physics point of view, it still dominates the market and will continue to do so for the next decades. The criteria for the more efficient performance of polycrystalline thin film PV devices over their single crystal counterpart is due to the grain boundaries enhancement supporting the collection of photogenerated minority carriers [13].There are indications that an electron barrier exists at the grain boundary, making devices fabricated from group II to VI compounds generally less sensitive than devices made from group IV materials. In the long term, new concepts of new classes of materials like organic solar or ¾ tendon size are great possibilities [14].

III. SINGLE-DIODE SOLAR CELL MODEL

A solar module is formed by combining solar cells, and an array is formed by connecting solar modules in series and parallel. Different authors refer to the single-diode model of solar cells, as shown in Fig. 1, from time to time to describe the PV and IV characteristics of cells against dynamically changed atmospheric conditions. The electric circuit of a single-diode model consists of a diode and a photogenerated current source (I_{ph}) and two resistances R_{sh} and one is in a series R_{se}which represent joules effect and recombination losses, respectively. The I-V and P-V characteristics can obtain the five parameters, series resistance, shunt resistance, diode ideality factor, photo-generated current, and reverse saturation current [15].

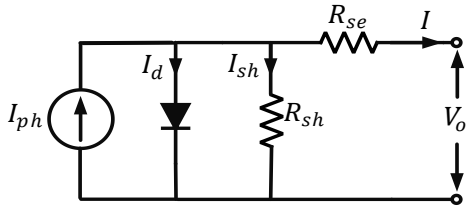

Figure 1 Single Diode Model of Solar Cell

The output current of the solar cell I is given by Eq. (1).

$$I = I_{ph} - I_d - I_{sh} \quad (1)$$

The output current I for a module is given in Eq. (2).

$$I = N_p \times I_{ph} - N_p \times I_o \left[exp\left(\frac{q(V + IR_{se})}{N_s \eta K T_O} \right) - 1 \right] - \frac{(V + IR_{se})}{R_{sh}} \quad (2)$$

Where $N_p$is the number of cells connected in parallel, N_sIs the number of cells connected in series, $I_d$is the diode current, q is the charge of an electron equal to 1.602 × 10^{-19} C, K is the Boltzmann's constant equal to 1.380 × 10^{-23} J/K, R_s is series resistance, η is the diode ideality factor, T_o is cell temperature, V is the output voltage of the solar cell and I is the output current of the cell.

The photogenerated current I_{ph} of the cell is given in Eq. (3)

$$I_{ph} = [I_{sc} + K_i(T_O - T_r)] \frac{G}{G_{ref}} \quad (3)$$

Where I_{sc} is short circuit current, K_iIs the short circuit current temperature coefficient, T_rIs reference temperature, G is real-time solar irradiance and G_{ref}Is irradiance at standard test conditions. The above equations clearly show that the solar cell outputs current. I depends upon the photogenerated current I_{ph}which is the function of solar irradiance and cell temperature? Any changes in either one, changes I_{ph}Ch affects the output current I and consequently, the output power POf the cell.

IV. SOLAR CELL PARAMETERS

A. Shunt Resistance (R_{sh})

Shunt resistance represents the conductivity of the current path across the solar cell junction and on the edges. Ideally, it is considered infinite for lossless cell structure [16]. It represents the parasitic loss due to impurities in PV material and damage to cell structure [17] [29][30]. At higher solar intensities, the shunt resistance becomes almost constant; at lower solar intensities, any increase in irradiance increases the shunt resistance [16,25]. A drop in shunt resistance with increases in solar intensity is also reported [26]. The shunt resistance decreases with increases in cell temperature [16,17].

B. Series Resistance (R_{se})

Series resistance represents a parasitic power-consuming parameter that affects a cell's efficiency and fill factor. It includes the resistance of cell contacts, bottom electrodes, bulk region, resistance of finger, etc. [18]. The series resistance of a PV cell cannot be eliminated but can be minimized by improving its design. The ideal value of series resistance is considered zero [19]. The series resistance drops with increases in solar intensities [25], and sometimes it remains almost constant with solar intensities [26]. It decreases linearly with increases in cell temperature [16], and increases in cell temperature are also reported [17].

C. Diode Ideality Factor(η)

The Diode Ideality Factor is the measurement of solar cell behavior close to a P-N junction device under illumination, which is the quality of the P-N junction [20]. A higher ideality factor value influences the device's open circuit voltage and fill factor [21]. Due to the aging factor, the useful life of solar cells is degraded, enhancing the ideality factor [22]. It drops sharply at a lower and higher solar intensity and decreases linearly [16,25]. In some cases, the diode ideality factor increases linearly with increases in solar irradiance [26]. It decreases with increases in cell temperature [16,17].

D. Reverse Saturation Current(I_o)

The reverse saturation current is due to the diffusion of minority charge carriers across the P-N junction. It depends upon the diffusion coefficient of the charge carrier and is affected by changes in temperature [23]. For lower solar intensity, any increase in irradiance drops the reverse saturation current very fast, and it becomes almost constant on higher irradiance change [25]. The linear increase in reverse saturation current with cell temperature and the exponential increase with cell temperature are also analyzed in different cases [17].

E. Photogenerated Current (I_{ph})

Photogenerated current is the rate of charge carrier generation by photons present in solar radiation [24]. It increases linearly with solar irradiance [16,25]. As temperature rises, photogenerated current increases rapidly [16,17].

V. METHODOLOGY

In this work, the MATLAB Simulink model of solar panels is taken to determine the changes in five electrical parameters at different values of temperatures and solar irradiance. For this purpose, the PV array block is taken, and specifications provided in the datasheet for standard test conditions (STC) are given as input. The performance curves (P-V and I-V) are obtained from standard test conditions for different temperatures at 1000 W/m² solar irradiance and different solar irradiances at 25°C operating temperature. It helps to observe the performance of solar panels for variable operating conditions. The change in P-V and I-V curves for 200 W/m² -1000 W/m² irradiance at 25°C temperature and P-V and I-V curves for 10 °C - 70°C temperature at 1000 W/m² irradiance are obtained and shown in Fig.4, 5, 6 and 7 respectively; these curves help to get the salient operating point. I_{mp}, V_{mp}, I_{sc} and V_{oc}. With the help of MATLAB PV array block, the change in five parameters of the single diode model, i.e., series resistance, shunt resistance, diode ideality factor, photo-generated current, and diode reverse saturation current, are observed with different operating conditions. This change in the above five parameters influences the solar cell's performance.

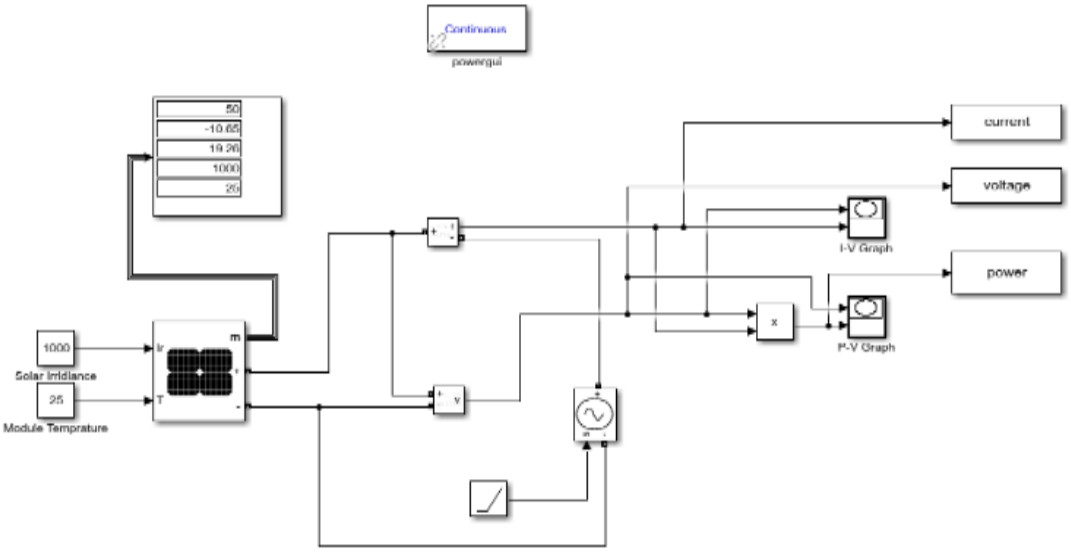

Figure 2 PV Model in MATLAB Simulink

In Fig.3, the P-V curve obtained at 1000 W/m² of irradiance and 25°C of temperature matches with the maximum power of datasheet value 300 Watts. With the change in temperature and irradiance, the P-V curve deviates from its standard test condition position. It is also clear from Fig. 4 that the open circuit voltage. V_{oc} A solar cell depends upon the temperature, and there is no significant change in short circuit current. I_{sc}. Similarly, the performance curves shown in Fig. 5 and 6 reveal that the maximum power occurs at constant temperature and variable solar irradiance. P_m and short circuit current I_{sc} changes and not a significant change in open circuit voltage V_{oc} Is observed. The datasheet values of P_m, I_{mp}, V_{mp}, I_{sc} and V_{oc}Match in the P-V and I-V curves shown in Fig. 3,4,5, and 6 at the standard test conditions.

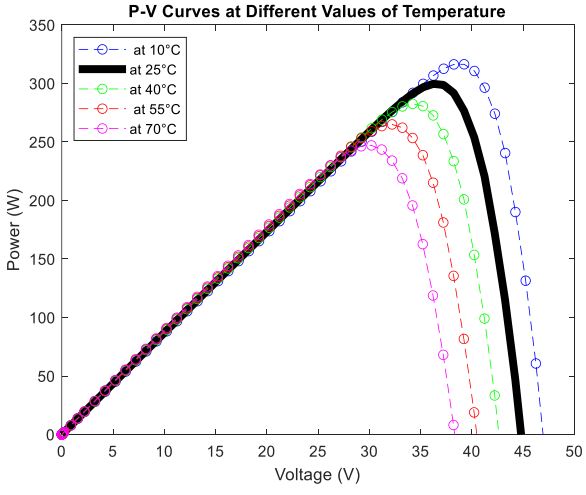

Figure 3 P-V Curve at Different Temperature

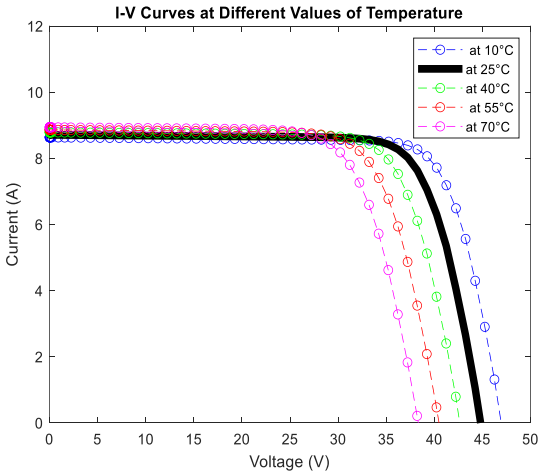

Figure 4 I-V Curve at Different Temperature

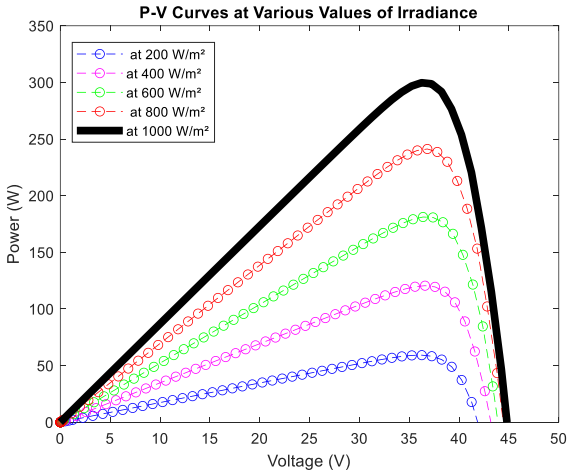

Figure 5 P-V Curve at Different Irradiance

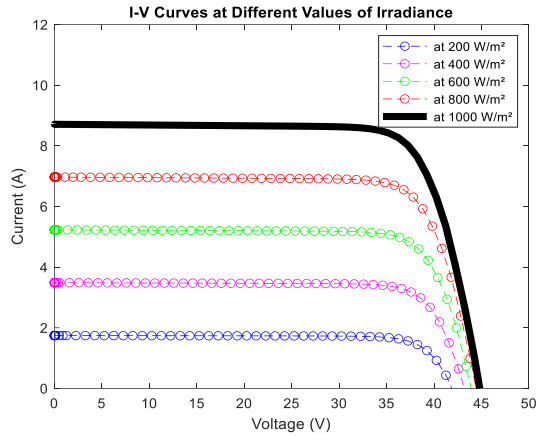

Figure 6 I-V Curve t Different Irradiance

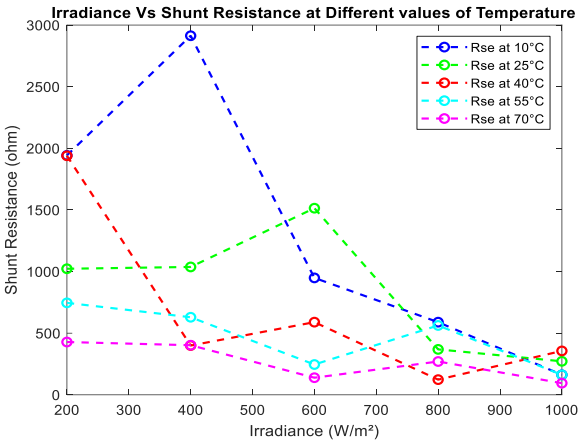

Figure 7 Irradiance vs. Shunt Resistance at Different T

Table I Tata TP 300 Series Solar Cell Datasheet

Parameters	Values
Maximum Power (P_{max})	300 W
Current in maximum power point (I_{mp})	8.20 A
Voltage in maximum power point (V_{mp})	36.6 V
Short circuit current (I_{sc})	8.71 A
Open circuit voltage (V_{oc})	44.8 V
Temperature coefficient of maximum power point (K_p)	-0.41 % / °C
Temperature coefficient of V_{oc} (K_v)	-0.32 % / °C
Temperature coefficient of I_{sc} (K_i)	0.058 % / °C
Number of series cell (N_s)	72

VI. RESULT AND DISCUSSION

The variation in five parameters of the single diode model of the photovoltaic module is analyzed here for different values of irradiance and temperature at standard test conditions. The irradiance range is between 200 W/m² to 1000 W/m², and the temperature range is between 10°C to 70°C. The impact of irradiance and temperature on the five electrical parameters of the single-diode model is given in Table II.

Table II

Shunt Resistance (R_{sh}) in ohms	271.7985
Series Resistance (R_s) in ohms	0.39329
Diode Ideality Factor (η)	0.94567
Reverse Saturation Current (I_o) in Ampere	6.7910e-11
Photogenerated Current (I_{ph}) in Ampere	8.8078

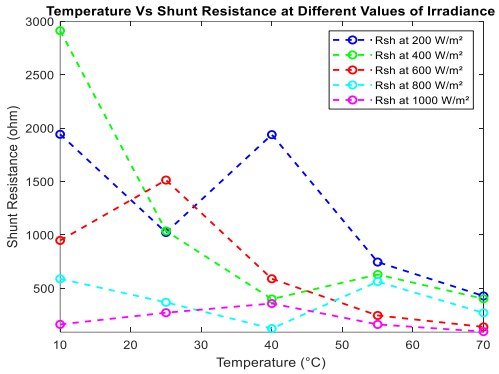

Figure 8 Temperature vs. Shunt Resistance at Different G

A. Shunt Resistance (R_{sh})

The solar irradiance has changed from 200 W/m² to 1000 W/m² for temperature values 10°C,25°C,40°C,55°C, and 70°C respectively. The solar irradiance has changed from 200 W/m² to 1000 W/m² for temperature values 10°C,25 °C,40°C,55°C, and 70 °C respectively. Fig.7 and Table III show that the shunt resistance R_{sh} decreases with increased irradiance at a constant temperature. From Fig. 8 and Table III, it is clear that as the temperature changes from 10°C to 70°C at each irradiance value, the shunt resistance R_{sh} decreases with the increase in temperature at constant irradiance.

TABLE III Values of Shunt Resistance in Ohms at Different Irradiance (G) and Temperature (T)

T (°C) → / G (W/m²) ↓	10°C	25°C	40°C	55°C	70°C
200	1942.6635	1022.7604	1939.5315	746.1096	428.3762
400	2913.2232	1037.4498	399.7871	629.3164	402.3473
600	948.6974	1514.1909	589.5477	245.8463	138.7799
800	589.3937	368.6567	123.195	562.7507	270.2530
1000	162.214	271.7985	358.0677	161.7902	94.4955

B. Series Resistance (R_{se})

From Fig.9, the change in series resistance R_s at solar irradiance 600 W/m² and above is insignificant for any operating temperature. It decreases significantly with temperatures of 40°C, 55°C, and 70°C in the range of 200 W/m² to 600 W/m² solar irradiance. Fig.10 shows that the series resistance R_s becomes high at higher temperatures at lower solar irradiance, that is, 200 W/m² and 400 W/m². For other irradiance values, the series resistance R_s does not change significantly with temperature change. The results of change in series resistance R_s are also tabulated in Table IV.

Retrieval Number: 100.1/ijrte.B808513020724
DOI: 10.35940/ijrte.B8085.13020724
Journal Website: www.ijrte.org

Published By:
Blue Eyes Intelligence Engineering and Sciences Publication (BEIESP)

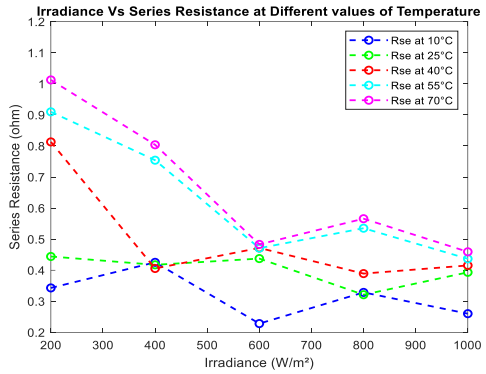

Figure 9 Irradiance vs. Series Resistance at Different T

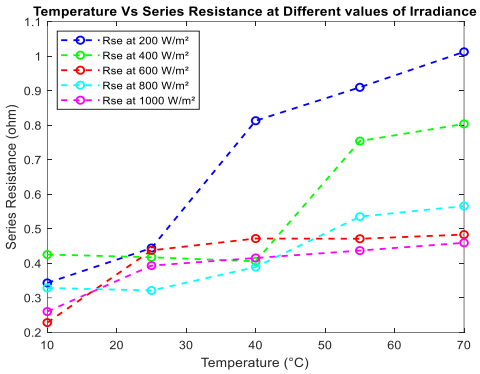

Figure 10 Irradiance vs. Series Resistance at Different G

TABLE IV Values of Series Resistance in Ohms at Different Irradiance (G) and Temperature (T)

T (°C) → / G (W/m²) ↓	10°C	25°C	40°C	55°C	70°C
200	0.34307	0.44429	0.81307	0.90985	1.01260
400	0.42542	0.41748	0.40568	0.75419	0.80384
600	0.22826	0.43754	0.47176	0.47110	0.48321
800	0.32867	0.32119	0.38922	0.53526	0.56592
1000	0.26021	0.39329	0.41546	0.43688	0.45935

C. Diode Ideality Factor (η)

Observation from Fig. 11 shows that when the solar irradiance increases for a constant value of temperature, the diode ideality factor η increases, and it decreases linearly with increases in operating temperature at a constant value of irradiance, as shown in Fig. 12. The change in diode ideality factor η with irradiance and temperature is tabulated in Table V.

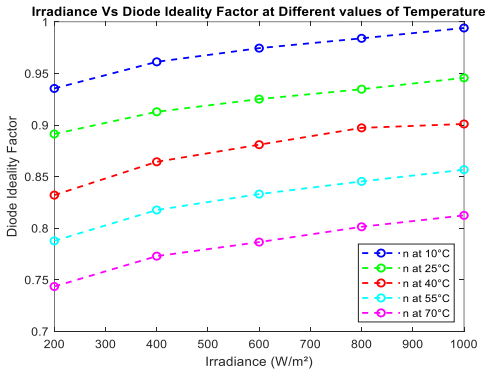

Figure 11 Irradiance vs Ideality Factor at Different T

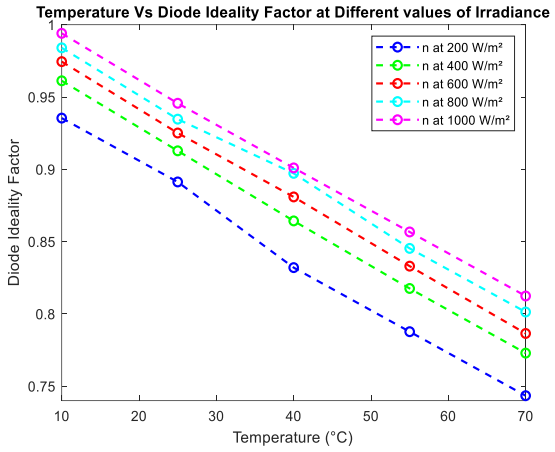

Figure 12 Irradiance vs. Ideality Factor at Different T

Table V Values of Diode Ideality Factor at Different Irradiance (G) and Temperature (T)

T (°C) → / G (W/m²) ↓	10°C	25°C	40°C	55°C	70°C
200	0.93542	0.89127	0.83202	0.78770	0.74344
400	0.96123	0.91279	0.86432	0.81759	0.77288
600	0.97448	0.92511	0.88090	0.83303	0.78647
800	0.98401	0.93468	0.89721	0.84531	0.80132
1000	0.99404	**0.94567**	0.90098	0.85668	0.81239

D. Reverse Saturation Current (I_o)

From Fig.13, it is clear that the reverse saturation current Io increases linearly with irradiance at a constant temperature value. The observation from Fig. 14 reveals that the reverse saturation current I_o remains almost constant with an increase in temperature at a constant irradiance. The change in reverse saturation current with irradiance and temperature is tabulated in Table VI.

Retrieval Number: 100.1/ijrte.B808513020724
DOI: 10.35940/ijrte.B8085.13020724
Journal Website: www.ijrte.org

Published By:
Blue Eyes Intelligence Engineering and Sciences Publication (BEIESP)

Table Vi Values of Reverse Saturation Current in Amperes at Different Irradiance (G) and Temperature (T)

T (°C) / G (W/m²)	10°C	25°C	40°C	55°C	70°C
200	1.3410e-11	1.3433e-11	1.3669e-11	1.3685e-11	1.3689e-11
400	2.6892e-11	2.6994e-11	2.7058e-11	2.7678e-11	2.7682e-11
600	3.9927e-11	4.0665e-11	4.0833e-11	4.0950e-11	4.1035e-11
800	5.3751e-11	5.3895e-11	5.4461e-11	5.5160e-11	5.5309e-11
1000	6.6627e-11	**6.7910e-11**	6.8073e-11	6.8351e-11	6.8596e-11

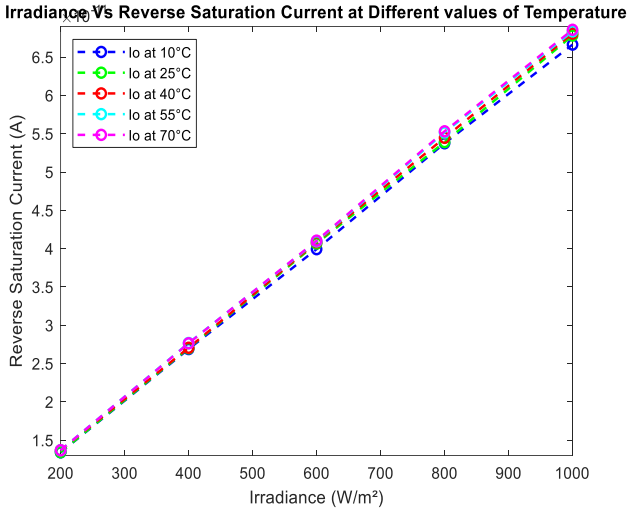

Figure 13 Irradiance vs Reverse Saturation Current at Different T

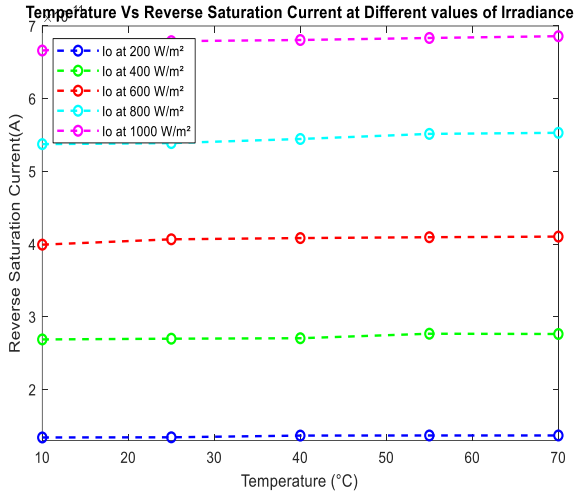

Figure 14 Irradiance vs Reverse Saturation Current at Different G

E. Photogenerated Current (I_{ph})

From Fig. 15, it is clear that the photogenerated current Iph increases linearly with irradiance at a constant value of temperature, and it remains constant for change in temperature at continual irradiance observed in Fig.16. The result of changes in photogenerated current is tabulated in Table VII.

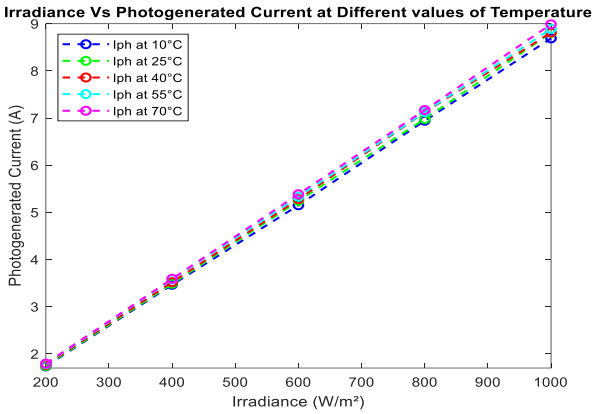

Figure 15 Irradiance vs Photogenerated Current at Different T

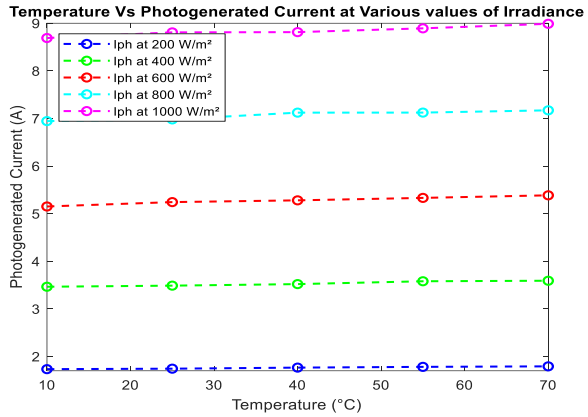

Figure 16 Irradiance vs Photogenerated Current Current at Different G

TABLE VII Values of Photogenerated Current in Amperes at Different Irradiance (G) and Temperature (T)

T (°C) / G (W/m²)	10°C	25°C	40°C	55°C	70°C
200	1.7342	1.7442	1.7666	1.7825	1.7931
400	3.4654	3.4883	3.5206	3.5805	3.5913
600	5.1511	5.2430	5.2799	5.3314	5.3854
800	6.9444	6.9798	7.1221	7.1230	7.1706
1000	8.6891	**8.8078**	8.8131	8.8926	8.9879

VII. CONCLUSION

This paper explores the single diode model of polycrystalline silicon solar cells to analyze the five electrical parameters, examining their variations in response to changes in temperature under standard test conditions using the MATLAB Simulink model.

Retrieval Number: 100.1/ijrte.B808513020724
DOI: 10.35940/ijrte.B8085.13020724
Journal Website: www.ijrte.org

Published By:
Blue Eyes Intelligence Engineering and Sciences Publication (BEIESP)

Observations reveal that the shunt resistance decreases with rising solar intensity and cell temperature and constant cell temperature and solar intensity, respectively. Similarly, the series resistance diminishes with increased solar intensity at 600 W/m² with constant cell temperature while exhibiting insignificant changes beyond this threshold. Conversely, the series resistance increases with increased cell temperature at constant irradiance. The observation shows the series resistance is higher at the lower value of solar intensity. The diode ideality factor demonstrates a notable increase with augmented solar irradiance at constant cell temperature while decreasing linearly with an increase in cell temperature at constant irradiance. The reverse saturation current exhibits a linear increase with elevated solar intensity at constant temperature, remaining constant at the increase in cell temperature at constant solar intensity. Furthermore, the photo-generated current linearly increases with heightened solar intensity at constant cell temperature, remaining constant at the increase in cell temperature at constant solar intensity. The increase in solar intensity increases the photo-generated current and improves the efficiency of solar cells. Various experiments have been conducted to analyze the five electrical parameters of the solar cell, employing different extraction methods. Still, no satisfactory results regarding the shunt and series resistance have been obtained. This paper presents an alternative approach, utilizing the MATLAB Simulink model to analyze the five electrical parameters of solar cells, yielding significantly improved results that align closer to the already reported results.

DECLARATION STATEMENT

Funding	No, we did not receive.
Conflicts of Interest	No conflicts of interest to the best of our knowledge.
Ethical Approval and Consent to Participate	No, the article does not require ethical approval and consent to participate with evidence.
Availability of Data and Material	Not relevant.
Authors Contributions	All authors having equal contribution for this article.

REFERENCE

1. S. Mohanty, P. K. Patra, S. S. Sahoo, and A. Mohanty, "Forecasting of solar energy with application for a growing economy like India: Survey and implication," *Renewable and Sustainable Energy Reviews*, vol. 78. Elsevier Ltd, pp. 539–553, 2017. doi: https://doi.org/10.1016/j.rser.2017.04.107
2. L. Ahmad, N. Khordehgah, J. Malinauskaite, and H. Jouhara, "Recent advances and applications of solar photovoltaics and thermal technologies," *Energy*, vol. 207, Sep. 2020, doi: https://doi.org/10.1016/j.energy.2020.118254
3. M. Hamada, M. Hojabri, S. Mekhilef, and H. M. Hamada, "Solar cell parameters extraction based on single and double-diode models: A review," *Renewable and Sustainable Energy Reviews*, vol. 56. Elsevier Ltd, pp. 494–509, Apr. 01, 2016. doi: https://doi.org/10.1016/j.rser.2015.11.051
4. T. Ahmad, S. Sobhan, and Md. F. Nayan, "Comparative Analysis between Single Diode and Double Diode Model of PV Cell: Concentrate Different Parameters Effect on Its Efficiency," *Journal of Power and Energy Engineering*, vol. 04, no. 03, pp. 31–46, 2016, doi: https://doi.org/10.4236/jpee.2016.43004
5. Benahmida, N. Maouhoub, and H. Sahsah, "An Efficient Iterative Method for Extracting Parameters of Photovoltaic Panels with Single Diode Model," 2020. https://doi.org/10.1109/REDEC49234.2020.9163858
6. D. S. H. Chan, J. R. Phillips, and J. C. H. Phang, "A COMPARATIVE STUDY OF EXTRACTION METHODS FOR SOLAR CELL MODEL PARAMETERS A Area," 1986.
7. X. Meng, F. Gao, and T. Xu, "A Hybrid Model Parameter Extraction Method for Single-Diode Model of PV Module," in *ECCE 2020 - IEEE Energy Conversion Congress and Exposition*, Institute of Electrical and Electronics Engineers Inc., Oct. 2020, pp. 3649–3653. doi: https://doi.org/10.1109/ECCE44975.2020.9235841
8. K. Chennoufi and M. Ferrari, "Parameters extraction of photovoltaic modules using a combined analytical-numerical method," in Proceedings of 2020 5th International Conference on Cloud Computing and Artificial Intelligence: Technologies and Applications, CloudTech 2020, Institute of Electrical and Electronics Engineers Inc., Nov. 2020. doi: https://doi.org/10.1109/CloudTech49835.2020.9365901
9. A. Senturk and R. Eke, "A new method to simulate the photovoltaic performance of crystalline silicon photovoltaic modules based on datasheet values," *Renew Energy*, vol. 103, pp. 58–69, Apr. 2017, doi: https://doi.org/10.1016/j.renene.2016.11.025
10. N. Asim *et al.*, "A review on the role of materials science in solar cells," *Renewable and Sustainable Energy Reviews*, vol. 16, no. 8. pp. 5834–5847, Oct. 2012. doi: https://doi.org/10.1016/j.rser.2012.06.004
11. D. Macdonald and A. Cuevas, "Reduced Fill Factors in Multicrystalline Silicon Solar Cells Due to Injection! Level Dependent Bulk Recombination Lifetimes," 1999. https://doi.org/10.1002/1099-159X(200007/08)8:4%3C363::AID-PIP328%3E3.3.CO;2-P J. W. Tringe and J. D. Plummer, "Electrical and structural properties of polycrystalline silicon," *J Appl Phys*, vol. 87, no. 11, pp. 7913–7926, 2000, doi: 10.1063/1.373475.
12. P. V Meyers and S. P. Albright, "Technical and Economic Opportunities for CdTe PV at the Turn of the Millennium." https://doi.org/10.1063/1.373475
13. L. M. Woods, G. Y. Robinson, D. H. Levi, and V. Kaydanov, "Electrical Characterization of Etched Grain-Boundary Properties from As-Processed px-CdTe Based Solar Cells Work performed under task number PV903101," 1998. [Online]. Available: http://www.doe.gov/bridge/home.html
14. Vinod, R. Kumar, and S. K. Singh, "Solar photovoltaic modeling and simulation: As a renewable energy solution," *Energy Reports*, vol. 4, pp. 701–712, Nov. 2018, doi: https://doi.org/10.1063/1.57996
15. E. Cuce, P. M. Cuce, and T. Bali, "An experimental analysis of illumination intensity and temperature dependency of photovoltaic cell parameters," *Appl Energy*, vol. 111, pp. 374–382, 2013, doi: https://doi.org/10.1016/j.egyr.2018.09.008
16. F. Ghani, G. Rosengarten, M. Duke, and J. K. Carson, "On the influence of temperature on crystalline silicon solar cell characterization parameters," *Solar Energy*, vol. 112, pp. 437–445, Feb. 2015, doi: https://doi.org/10.1016/j.apenergy.2013.05.025
17. M. Sabry and A. E. Ghitas, "Influence of temperature on methods for determining silicon solar cell series resistance," *Journal of Solar Energy Engineering, Transactions of the ASME*, vol. 129, no. 3, pp. 331–335, Aug. 2007, doi: https://doi.org/10.1016/j.solener.2014.12.018
18. K. C. Fong, K. R. McIntosh, and A. W. Blakers, "Accurate series resistance measurement of solar cells," *Progress in Photovoltaics: Research and Applications*, vol. 21, no. 4, pp. 490–499, Jun. 2013, doi: https://doi.org/10.1115/1.2735350
19. H. Bayhan and M. Bayhan, "A simple approach to determine the solar cell diode ideality factor under illumination," *Solar Energy*, vol. 85, no. 5, pp. 769–775, May 2011, doi: https://doi.org/10.1002/pip.1216
20. F. Babbe, L. Choubrac, and S. Siebentritt, "The Optical Diode Ideality Factor Enables Fast Screening of Semiconductors for Solar Cells," *Solar RRL*, vol. 2, no. 12, Dec. 2018, doi: https://doi.org/10.1016/j.solener.2011.01.009
21. C. M. A. da Luz, F. L. Toffoli, P. dos Santos Vicente, and E. M. Vicente, "Assessment of the ideality factor on the performance of photovoltaic modules," *Energy Convers Manag*, vol. 167, pp. 63–69, Jul. 2018, doi: https://doi.org/10.1002/solr.201800248
22. A. D. Dhass, Y. Prakash, and K. C. Ramya, "Effect of temperature on internal parameters of a solar cell," in *Materials Today: Proceedings*, Elsevier Ltd, Jan. 2020, pp. 732–735. doi: https://doi.org/10.1016/j.enconman.2018.04.084
23. P. Ferrada *et al.*, "Potential for photogenerated current for silicon-based photovoltaic modules in the Atacama Desert," *Solar Energy*, vol. 144, pp. 580–593, 2017, doi: https://doi.org/10.1016/j.matpr.2020.06.079

24. F. Khan, S. N. Singh, and M. Husain, "Effect of illumination intensity on cell parameters of a silicon solar cell," in *Solar Energy Materials and Solar Cells*, Sep. 2010, pp. 1473–1476. doi: https://doi.org/10.1016/j.solener.2017.01.053
25. M. Chegaar, A. Hamzaoui, A. Namoda, P. Petit, M. Aillerie, and A. Herguth, "Effect of illumination intensity on solar cells parameters," in *Energy Procedia*, Elsevier Ltd, 2013, pp. 722–729. doi: https://doi.org/10.1016/j.solmat.2010.03.018
26. Rajaram, R. S., & Victor, K. (2020). Validation of Shadow Effects on Solar Photovoltaic Modules Based on Module Positioning. In International Journal of Innovative Technology and Exploring Engineering (Vol. 9, Issue 3, pp. 1017–1022). https://doi.org/10.35940/ijitee.c7989.019320
27. Kumar, Dr. A., Anand, Dr. G., & Sahoo, Dr. A. K. (2019). Going Solar-Conducive Shift to Domestic Solar Electric System. In International Journal of Recent Technology and Engineering (IJRTE) (Vol. 8, Issue 4, pp. 11615–11620). https://doi.org/10.35940/ijrte.d9045.118419
28. Agarwal, V., Jain, Dr. S., & Jindal, Dr. S. (2019). Design of Solar Energy based Hybrid Community Cooking System. In International Journal of Engineering and Advanced Technology (Vol. 9, Issue 1, pp. 3101–3107). https://doi.org/10.35940/ijeat.e7360.109119
29. Sharma, R., Sharma, S., & Sharma, S. (2020). Techno-Economic Analysis of Solar Powered Water Pumping System. In International Journal of Soft Computing and Engineering (Vol. 9, Issue 5, pp. 24–32). https://doi.org/10.35940/ijsce.e3343.019520
30. Kumar, R. R. (2022). Heat Transfer Analysis of Advanced Solar Collector. In Indian Journal of Energy and Energy Resources (Vol. 1, Issue 4, pp. 1–4). https://doi.org/10.54105/ijeer.d1026.081422

AUTHORS PROFILE

Chandrashekhar Pardhi is pursuing an M.E. degree (M.Tech.) in High Voltage and Power System (HVPS) Engineering from Jabalpur Engineering College, Jabalpur. His area of interest is Renewable energy sources and the application of power converters in solar-powered systems.

Kanchan Khare – She completed her B.Sc. and M.Sc. degree in applied chemistry from Govt. M.H. college Jabalpur. After that, she completed a Ph.D. in polymer chemistry at Govt. Science College Jabalpur. She is an associate professor in the Department of Applied Chemistry at Jabalpur Engineering College, Jabalpur. Her areas of research interest are Polymer Chemistry, Nano Science, and Green Energy. She has published many research articles in international and national journals.

Ashish Choubey completed his B.E. in electrical engineering from BIT, Durg. After that, he completed an M. Tech in Power Electronics from SGSITS Indore. He is pursuing a Ph.D. in power and control from IIITDM, Jabalpur. He works as an Assistant Professor in the Electrical Engineering Department at Jabalpur Engineering College, Jabalpur. His research interests are Renewable energy, DC-DC Converters, and their Control.